Journal of Applied Physics

Site-selective spectroscopy of Ho^{3+}:KYF_4

Cite as: Journal of Applied Physics **75**, 502 (1994); https://doi.org/10.1063/1.355829
Submitted: 23 August 1993 . Accepted: 23 September 1993 . Published Online: 17 August 1998

R. E. Peale, H. Weidner, P. L. Summers, and B. H. T. Chai

Site-selective spectroscopy of Ho^{3+}:KYF_4

R. E. Peale, H. Weidner, and P. L. Summers
Department of Physics, University of Central Florida, Orlando, Florida 32816

B. H. T. Chai
Center for Research and Education in Optics and Lasers, University of Central Florida, Orlando, Florida 32816

(Received 23 August 1993; accepted for publication 23 September 1993)

Site-selective photoluminescence spectroscopy of Ho^{3+} ions in single-crystal KYF_4, measured with a Fourier-transform spectrometer at 80 and 2 K sample temperatures, gives evidence for two dissimilar classes of crystal-field sites. Three similar sites contribute to each class giving a total of six sites in agreement with recent crystallographic results. Analysis of crystal-field splittings indicates that only one of the classes can contribute to Yb→Ho upconversion green lasing in (Yb,Ho):KYF_4.

I. INTRODUCTION

In crystals doped both with Yb^{3+} and Ho^{3+} ions, sequential Yb→Ho energy transfer gives rise to infrared-pumped green luminescence. Lasing by this mechanism has been realized in BaY_2F_8 at 77 K.[1] Renewed interest in upconversion lasing systems reflects the development of powerful strain-layered InGaAs laser diodes, which can directly pump the 1 μm absorption of Yb^{3+}. Potential compact all-solid-state green lasers have applications in biology, medicine, and optical data storage. The need for practical devices operating at room temperature drives the continued investigation of upconversion in new crystals.

We recently reported[2-4] that room-temperature Yb→Ho upconversion lasing is more likely in the new crystal KYF_4(KYF) than in BaY_2F_8(BYF). Upconversion lasing at 77 K has since been observed in (Yb,Ho):KYF.[5] KYF is a multisite crystal, as shown for Ho^{3+} by absorption[2] and by site-selective photoluminescence for[6] Gd and[7] Nd dopants. However, the number of sites found differs in each study. All disagree with the number predicted by the crystal structure, as determined by x-ray crystallography,[8] which clearly indicates six substitutional sites divided evenly between two dissimilar types. Since neither site-selective study is relevant to Yb→Ho energy transfer, the number and characteristics of the sites which contribute to lasing remains in question.

We present here the first site-selective study of Ho^{3+} in KYF. We find two classes of photoluminescence with three sites contributing to each class, in agreement with the structural work. A significant difference in the degree of crystal-field splitting is found for the two classes. We find that only one class possesses Stark splitting favorable for Yb→Ho upconversion lasing.

II. EXPERIMENT

Large, optical quality, single crystals of KYF were grown by the top-seeded solution technique. The sample studied here was doped with Ho^{3+} at 0.4 at. % in the melt.

The absorption and photoluminescence were measured using a Bomem DA8 Fourier spectrometer. Measurements at 80 K made use of a homebuilt liquid-nitrogen cold finger cryostat. Measurements at 2 K were performed with a Janis supervaritemp liquid-helium cryostat. Photoluminescence was excited using a cw Coherent Ar-laser pumped dye laser with DCM dye. The light path for both absorption and luminescence is entirely in vacuum, so frequencies are in vacuum wave numbers. Laser light scattered into the spectrometer was filtered out before the Si or InSb detector using a Schott RG780 long-pass filter. For one special measurement, Schott filter RG645 was used (see below). The scattered laser light was separately measured by the Fourier spectrometer to determine excitation frequencies (also in vacuum wavenumbers). The dye-laser linewidth varied from 1 to 4 cm^{-1} for different positions of the birefringent tuning plate.

III. RESULTS

Figure 1 is a schematic energy level diagram which shows the free Ho^{3+} terms and the optical transitions studied in this paper. The $^5I_8 \rightarrow {}^5F_5$ absorption transitions, shown by the upward arrow, are pumped with the tunable dye laser. The resulting photoluminescence is indicated by downward arrows. Upconversion in Ho^{3+} by energy transfer from excited Yb^{3+} ions proceeds by the sequential excitations $^5I_8 \rightarrow {}^5I_6 \rightarrow {}^5F_4$, $^5S_2$. This is followed by optical relaxation to the ground term with emission of green light.

Figure 2 presents the $^5I_8 \rightarrow {}^5F_5$ transmission spectrum at a sample temperature of 1.7 K. The instrumental resolution was 1.5 cm^{-1}. (The derivative like feature at 15 798 cm^{-1} is an artifact of visible Fourier spectroscopy due to scattered HeNe laser radiation from the dynamic alignment system of the spectrometer.) Only a few additional lines appear at 80 K from thermal population of Stark levels in the $^5I_8$ term. These lines are located on the low-frequency end of Fig. 2 and are very weak, which indicates a large separation between the lowest two levels in the ground term. The DCM-dye laser can be tuned across the frequency range of Fig. 2. Excitation above 15 700 cm^{-1} produces a characteristic luminescence spectrum, which we designate Class I. Excitation below 15 730 cm^{-1} produces bands which differ from Class I with respect to frequencies and intensities of individual lines. We designate this second type of luminescence Class II. The

 0021-8979/94/75(1)/502/5/$6.00

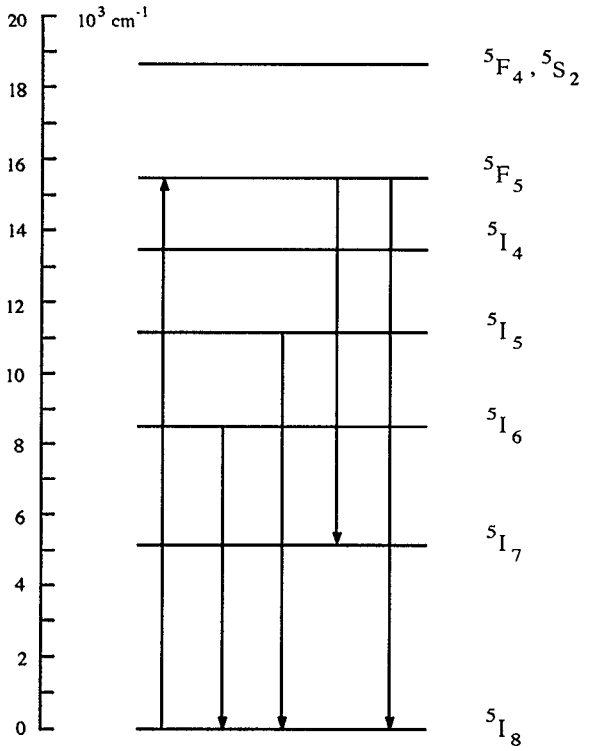

FIG. 1. Schematic energy level diagram for Ho^{3+} ions. The dye-laser pumping and the four photoluminescence bands studied in this work are indicated by arrows.

pumping regions for each class are indicated at the top of Fig. 2. They overlap slightly.

Figure 3 presents $^5F_5 \rightarrow {}^5I_7$ photoluminescence for two different excitation frequencies. The upper spectrum was excited at 15 913 cm^{-1}, which is within the strong line at highest frequency in Fig. 2. The lower spectrum was excited at 15 674 cm^{-1}, which is within a strong band near the center of Fig. 2. It is clear that the two spectra are very different, and they are designated Class I and II, accordingly.

Figure 4 presents $^5I_5 \rightarrow {}^5I_8$ photoluminescence at 80 K with excitation at 15 903 cm^{-1} (upper, Class I) and 15 682 cm^{-1} (lower, Class II). Again, the two classes are distinctly different. Only one line is coincident. Lines at the high-frequency end tend to be sharp and reveal much detail.

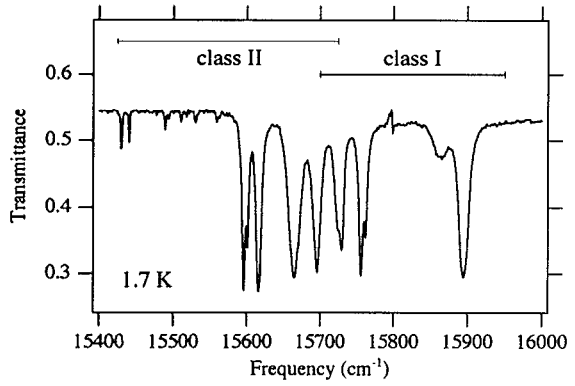

FIG. 2. Transmittance spectrum for Ho^{3+} $^5I_8 \rightarrow {}^5F_5$ transitions in KYF_4. The sample temperature was 1.7 K.

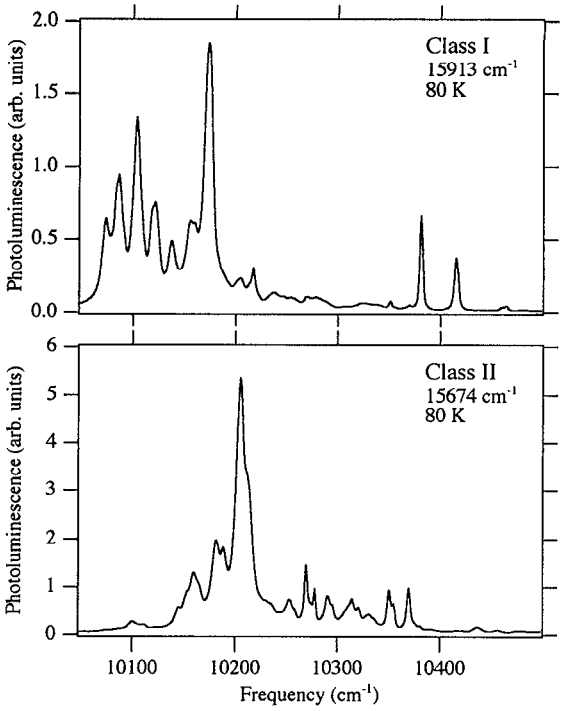

FIG. 3. Ho^{3+}:KYF_4 $^5F_5 \rightarrow {}^5I_7$ photoluminescence spectra. The sample temperature and pumping frequencies are indicated.

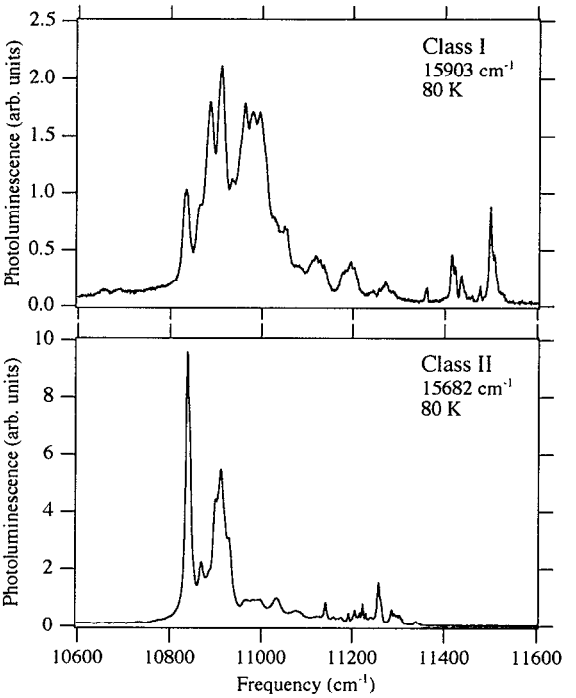

FIG. 4. Ho^{3+}:KYF_4 $^5I_5 \rightarrow {}^5I_8$ photoluminescence spectra. The sample temperature and pumping frequencies are indicated.

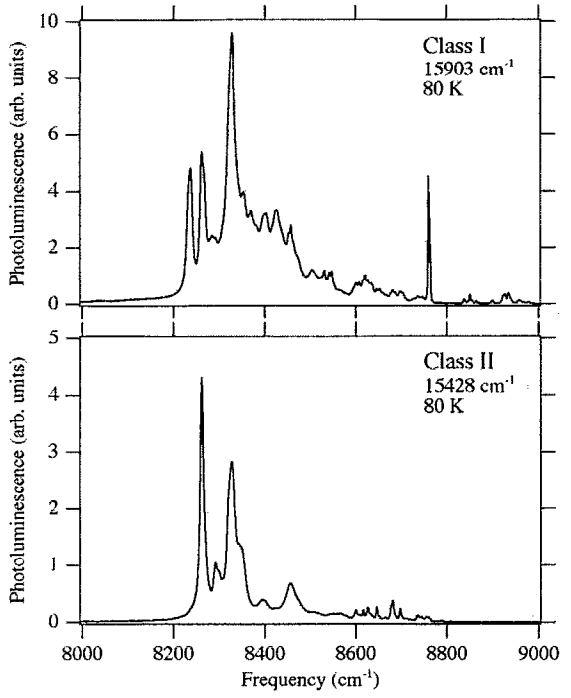

FIG. 5. Ho^{3+}:KYF_4 $^5I_6 \rightarrow {}^5I_8$ photoluminescence spectra. The sample temperature and pumping frequencies are indicated.

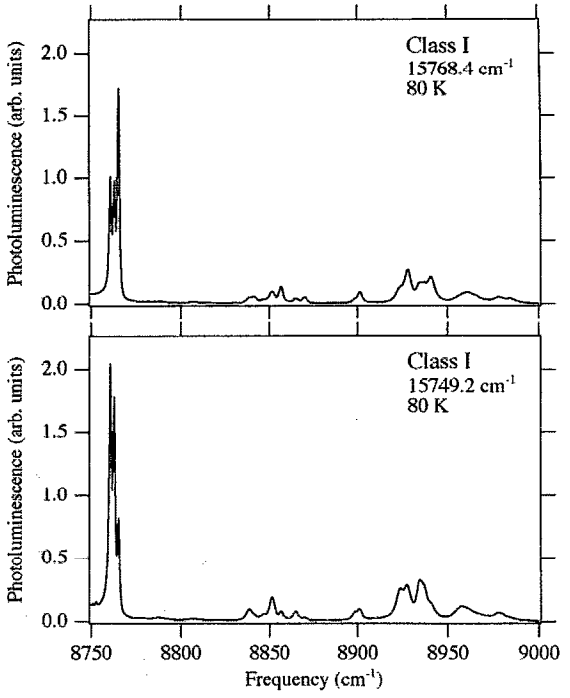

FIG. 6. High-frequency region of Class I Ho^{3+}:KYF_4 $^5I_6 \rightarrow {}^5I_8$ photoluminescence spectra. The sample temperature and pumping frequencies are indicated.

Figure 5 presents the $^5I_6 \rightarrow {}^5I_8$ photoluminescence band at 80 K with excitation at 15 903 cm^{-1} (upper, Class I) and at 15 428 cm^{-1} (lower, Class II). Again, the two distinct classes appear with just a single coincident line. Also, the features at higher frequency are sharper and more structured for both classes.

For the three photoluminescence bands presented in Figs. 3–5, the division into two classes follows the division of the pumping band indicated in Fig. 2. This has been verified by tuning the laser through the frequency range of Fig. 2. In the region of the overlap, both classes of luminescence are strong in the spectra. A common characteristic of the three bands presented in Figs. 3–5 is the larger frequency span of Class I: Lines are found at both higher and lower frequencies for Class I than for Class II.

Figure 6 presents the higher-frequency region of Class I $^5I_6 \rightarrow {}^5I_8$ photoluminescence at 80 K for two slightly different excitation frequencies. A resolution of 0.5 cm^{-1} was necessary to resolve the sharp triplet of lines on the low-frequency end. The relative strength of the three lines differs in the two spectra, and correlated changes are observed in the weaker bands at higher frequency. The various Class I lines which increase or decrease together as the excitation is tuned can be divided into three and only three different independent groups. These correlated changes have been analyzed for 40 different pumping frequencies covering the range for Class I indicated in Fig. 2. These observations indicate that three similar but spectroscopically distinct sites contribute to Class I photoluminescence.

Figure 7 presents the high-frequency region of Class II $^5I_6 \rightarrow {}^5I_8$ photoluminescence at 80 K for two slightly differ-

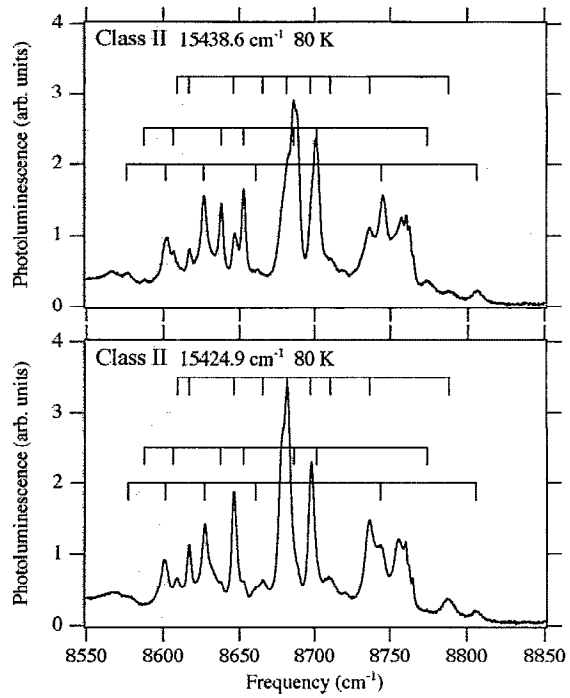

FIG. 7. High-frequency region of Class II Ho^{3+}:KYF_4 $^5I_6 \rightarrow {}^5I_8$ photoluminescence spectra. The sample temperature and pumping frequencies are indicated.

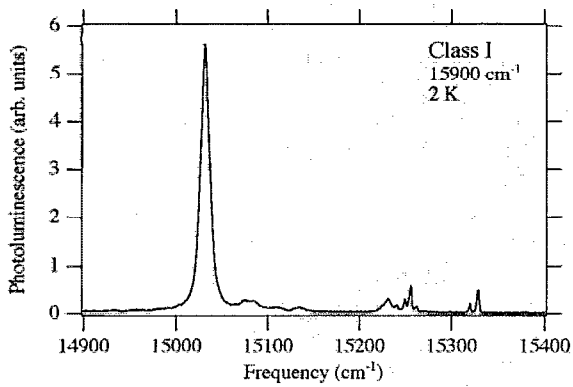

FIG. 8. Class I $^5F_5 \rightarrow {}^5I_8$ photoluminescence at 2 K sample temperature and 1 cm^{-1} resolution. The highest-frequency lines of this band are cut out by the long-pass filter used to attenuate the 15 900 cm^{-1} scattered excitation-laser light.

ent excitation frequencies. Division of the observed lines among three groups is indicated above them by connected vertical bars. These three groups of lines increase and decrease independently with changes in pump frequency. Lines within a group always maintain their relative strengths. This grouping is observed consistently for more than 50 different pumping frequencies spanning the Class II range indicated in Fig. 2. We conclude that three sites contribute to Class II emission.

Analysis of the $^5I_5 \rightarrow {}^5I_8$ and $^5F_5 \rightarrow {}^5I_7$ photoluminescence bands, which are measured simultaneously with the $^5I_6 \rightarrow {}^5I_8$ band, yields identical conclusions: Three sites contribute to each of the two classes, yielding a total of six sites.

Figure 8 presents Class I $^5F_5 \rightarrow {}^5I_8$ photoluminescence at a sample temperature of 2 K and a resolution of 1 cm^{-1}. The purpose of this measurement was to determine the Class I ground-term splitting, as discussed below. This band is very close in frequency to the laser light used to excite it. Laser light that scatters into the spectrometer must be attenuated by careful optical filtering in order to obtain adequate signal to noise in the luminescence spectrum of interest. Discontinuities in cutoff frequencies for commercially available long-pass filters prevent measurements of this band at all excitation frequencies. In particular, our Class II $^5F_5 \rightarrow {}^5I_8$ spectra were of poor quality, but were distinctly different from the Class I spectrum in Fig. 8.

IV. DISCUSSION AND SUMMARY

The observed frequency ranges of Class I and Class II luminescence permit us to evaluate specific energy parameters relevant to Yb→Ho upconversion lasing. Minimum and maximum photoluminescence frequencies are given in Table I. Figure 2 reveals that $^5F_5$ Class I levels have a higher "center of gravity" than Class II levels. This holds for $^5I_5$ and $^5I_6$ terms as well, as we will demonstrate, giving the schematic level diagram Fig. 9. The levels given in Fig. 9 were determined from our data as follows.

TABLE I. Minimum and maximum photoluminescence line-center frequencies (cm^{-1}) for Ho^{3+} in KYF_4 at 80 K.

Band	Class	Minimum	Maximum
$^5I_6 \rightarrow {}^5I_8$	I	8230	8984
	II	8262	8805
$^5F_5 \rightarrow {}^5I_7$	I	10 074	10 464
	II	10 100	10 455
$^5I_5 \rightarrow {}^5I_8$	I	10 830	11 529
	II	10 838	11 345
$^5F_5 \rightarrow {}^5I_8$	I	15 030	
	II	15 075	

For both classes, upper levels of the $^5I_5$ and $^5I_6$ terms are found from their highest frequency 80 K emission to the ground term $^5I_8$. This determination requires thermal population of the highest Stark level in the initial terms. The Class I values are equal to the frequencies of the highest absorption lines for the corresponding terms,[2] which verifies that the highest levels in each term belong to Class I. Upper $^5F_5$ levels are determined from the class-selective excitation; the Class I value equals the position of the highest $^5F_5$ absorption line, as shown in Fig. 2.

Lower Class II levels are found from the lowest line for each term in the 1.7 K absorption spectra.[2] The lower Class I $^5F_5$ level was determined from the class-selective excitation, as indicated in Fig. 2. Lower Class I levels indicated in Fig. 8 by *b*, *c* were not determined in this work.

Two important parameters for Ho^{3+} lasing in the green are the ground-term splittings Δ_I and Δ_{II}. For efficient lasing, they need to be large because the ground term contains the final states for Ho^{3+} green emission. The parameter Δ_{II} is determined from the minimum Class II luminescence transitions, indicated by downward arrows, and from the lower levels of the initial terms. The transitions from $^5F_5$, $^5I_5$, and $^5I_6$ give the values 355, 356, and 356 cm^{-1}, respectively. The consistency of these three values verifies that the lowest levels for the three terms belong to Class II.

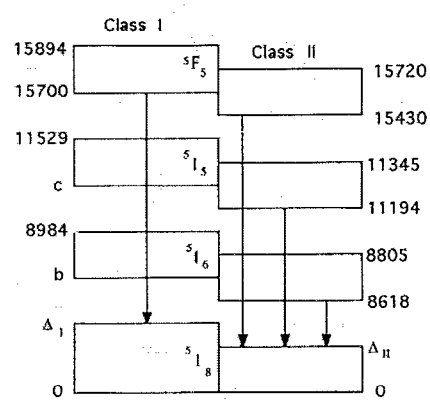

FIG. 9. Schematic energy diagram showing relative Stark splittings for two classes in Ho^{3+}:KYF. Energies are not to scale and some terms are left out for clarify. Determination of level positions is discussed in the text. Downward arrows show transitions used to derive ground-term splittings.

The parameter Δ_I is determined from the minimum frequency 2 K $^5F_5 \rightarrow {}^5I_8$ luminescence plotted in Fig. 8. This transition is indicated by a downward arrow in Fig. 9. With a lowest Class I $^5F_5$ level of 15 700 cm^{-1}, we obtain a value for Δ_I of 670 cm^{-1}. (In principle, it should be possible to read off the value of Δ_I directly from the spread of emission frequencies in Fig. 8. However the high-frequency $^5F_5 \rightarrow {}^5I_8$ emission is strongly suppressed by the Schott RG645 long-pass filter used to attenuate the scattered 15 900 cm^{-1} laser radiation at the detector. This filter has a transmittance which varies from 0.9 to 0.6 over the range plotted in Fig. 8. At 15 700 cm^{-1}, where the highest 2 K emission line is expected, the filter transmittance is less than 0.1. No lines emerge from the noise above the range plotted in Fig. 8.)

The parameter Δ_{II} is rather small, being about 60 cm^{-1} less than the ground term splitting for Ho^{3+} in BYF.[2] Class II Ho^{3+}:KYF is therefore less suited for room-temperature green lasing than is Ho^{3+}:BYF. We note that Δ_{II} is quite close to the 341 cm^{-1} splitting found in Ho^{3+}:YLF, for which upconversion green lasing is unknown. In contrast, Δ_I is quite large, being more than three times kT at room temperature and 257 cm^{-1} larger than the ground-term splitting of Ho^{3+} in BYF.

A second parameter of relevance to upconversion lasing is the energy mismatch at the first Yb→Ho transfer step. The difference between the minimum Yb^{3+} luminescence and maximum Ho^{3+} $^5I_8 \rightarrow {}^5I_6$ absorption (always positive) should be small to limit the number of phonons required to assist the transfer. For the minimum Yb^{3+} luminescence in KYF, we find[9] the value 9690 cm^{-1}. This gives an energy mismatch of 706 cm^{-1} for Class I and 885 cm^{-1} for Class II. Both mismatch values are less than the 1055 cm^{-1} found for (Yb,Ho):BYF, and this favors KYF over BYF. The value for Class I is less than that for Class II, giving Class I the advantage again.

The published crystal structure[8] permits us to make tentative assignments for the two classes of emission to the two types of local environments in KYF. The F_7 cages surrounding the Y^{3+} sites (the dopant sites) are described as either monocapped trigonal prisms (type I) or a pentagonal bi-pyramids (type II). Type I is the more distorted with both larger and smaller Y^{3+} to F^- distances present. Also, the average distance to nearest neighbor F^- ions is slightly less for type I. These two observations suggest that the Stark splitting for ions at type I sites will be greater and have higher center of gravity than ions at type II sites. Hence, we conclude that Class I photoluminescence arises from Ho^{3+} ions which occupy type I sites.

The crystal structure further shows that Class II Ho^{3+} ions are likely to be active quenching centers. Type I and type II sites alternate in a chain. Adjacent type I and type II F_7 cages are edge bonded, which is a favorable situation for energy transfer. Therefore, at Ho^{3+} concentrations sufficient to populate neighboring sites, Class II Ho^{3+} ions may parasitically drain energy from the laser-active Class I centers.

In summary, we have presented evidence that there are six sites in KYF_4 divided equally into two classes. Energy parameters for Ho^{3+} determined from site-selective photoluminescence show that only one of the classes is favorable for upconversion lasing. We postulate that the favorable sites are those described as monocapped trigonal prisms, while the unfavorable, perhaps parasitical, sites are those described as pentagonal bi-pyramids.

ACKNOWLEDGMENT

REP thanks the University of Central Florida (UCF) Division of Sponsored Research for generous start up funds.

[1] L. F. Johnson and H. J. Guggenheim, Appl. Phys. Lett. **19**, 44 (1971).
[2] R. E. Peale, H. Weidner, P. L. Summers, X. X. Zhang, M. Bass, and B. H. T. Chai, *OSA Proceedings on Advanced Solid-State Lasers*, edited by A. A. Pinto and T. Y. Fan (Optical Society of America, Washington, DC, 1993), Vol. 15, pp. 450–453.
[3] X. X. Zhang, M. Bass, B. H. T. Chai, and R. E. Peale, *OSA Proceedings on Advanced Solid-State Lasers*, edited by A. A. Pinto and T. Y. Fan (Optical Society of America, Washington, DC, 1993), Vol. 15, pp. 253–257.
[4] X. X. Zhang, M. Bass, and B. H. T. Chai, *OSA Proceedings on Advanced Solid-State Lasers*, edited by A. A. Pinto and T. Y. Fan (Optical Society of America, Washington, DC, 1993), Vol. 15, pp. 454–458.
[5] R. J. Thrash, R. H. Jarman, B. H. T. Chai, and A. Pham, accepted for presentation at the Conference on Compact Blue-Green Lasers, Feb. 10–11, 1994, Salt Lake City; R. J. Thrash, Amoco Technology Company, P. O. Box 3011, Naperville, IL 60566, (703) 420-4695 (private communication 1993).
[6] J. Sytsma, S. J. Kroes, G. Blasse, and N. M. Khaidukov, J. Phys.: Condens. Matter **3**, 8959 (1991).
[7] Y. Yamaguchi, K. M. Dinndorf, H. P. Jenssen, and A. Cassanho, *OSA Proceedings on Advanced Solid-State Lasers*, edited by A. A. Pinto and T. Y. Fan (Optical Society of America, Washington, DC, 1993), Vol. 15, pp. 36–40.
[8] Y. Le Fur, N. M. Khaidukov, and S. Aléonard, Acta Cryst. **C48**, 978 (1992).
[9] A. Rapaport, H. Weidner, and R. E. Peale (unpublished) (1993).